Coherence Cube and beyond

Satinder Chopra[1]

Introduction

Coherence Cube technology was released to the world geophysical community by Amoco Production Research in 1995 (Bahorich & Farmer 1995). The Coherence Cube is essentially a cube of coherence coefficients generated from the input 3D seismic data volume, that portrays faults and other stratigraphic anomalies clearly, on time or horizon slices. These images show up distinctly, depicting buried deltas, river channels, reefs, etc. Traditional seismic time slices are an alternative approach, often used for interpreting faults that run perpendicular to strike. However, when faults run parallel to strike, they become difficult to interpret as fault lineaments become superimposed on bedding lineaments. Similarly, the remarkable detail of stratigraphic features such as river channels, mud flows and submarine canyons are unidentifiable, even under close scrutiny.

Coherence measurements in three dimensions represent the trace-to-trace similarity and therefore produce interpretable changes in these cases. Similar traces are mapped with high coherence coefficients, while discontinuities have low coefficients. Regions of seismic traces cut by faults, for example, result in sharp discontinuities of trace-to-trace coherence, resulting in delineation by low coherence along fault planes. Since the three-dimensionality is an essential ingredient of coherence computation, faults or fractures in any orientation are revealed equally well. Figure 1 depicts an example from offshore East Coast of Canada where NW–SE faults and fractures, apparently difficult to interpret, show up clearly on the coherence slice. Overlays of coherence slices on a seismic slice greatly help in interpretation (Fig. 1c).

Stratigraphic features generate similar discontinuities, resulting in a sharp delineation of reef and channel boundaries (Figs 2 and 3) and deltaic sediments. Consequently, in addition to faults, channels and beaches, the coherence cube has been successfully used for the easy visualization of mud volcanoes, mass wasting, dewatering features, etc. An attractive characteristic of the coherence cube is that it gives an unbiased view of the features in the seismic volume. No interpretation is required for viewing them.

Since the introduction of the coherence cube to the world in 1995 (Bahorich & Farmer 1995), the technology has been constantly upgraded by means of more refined algorithms, displays, applications and methodologies, aimed at extracting more meaningful detail that would not only aid the interpreter but also improve accuracy and time effectiveness.

Algorithms

Different statistical measures are used for computing the coherence values. All coherence measures should be calculated along some estimate of reflector dip. The original coherence algorithm (Bahorich & Farmer 1995) used time-lagged cross-correlation to estimate the apparent dips in the in-line and cross-line directions. An estimate of coherence can then be obtained by combining the cross-correlation coefficients along these two apparent dips. We then generate a cube of 3D coherence by continuing this process for all samples and all traces in the volume.

The second-generation coherence algorithm used semblance as a coherence estimate (Marfurt *et al.* 1998). In this implementation, we begin by defining a spatial aperture consisting of five or more traces and one or more samples centred about each analysis point in the input cube. Within each analysis window we next calculate the semblance along a suite of postulated planar reflectors, each of which is given by a user-defined dip/azimuth. We define the instantaneous dip/azimuth as that dip/azimuth corresponding to the planar reflector having maximum semblance. Depending on our interpretational objectives, we may choose to obtain a more robust estimate of reflector dip/azimuth through the use of 3D mean, median or alpha-trim mean filters. We define seismic coherence as the semblance calculated along the dip of the seismic

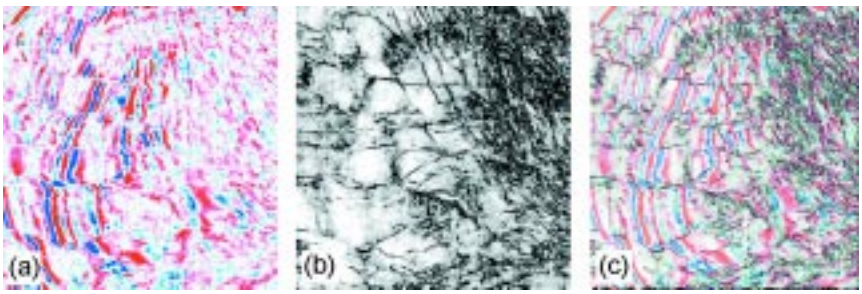

Figure 1 Coherence slice not only reveals faults with clarity but also the intensively fractured region to the right.

[1]Scott Pickford, Calgary. E-mail: schopra@scopica.com

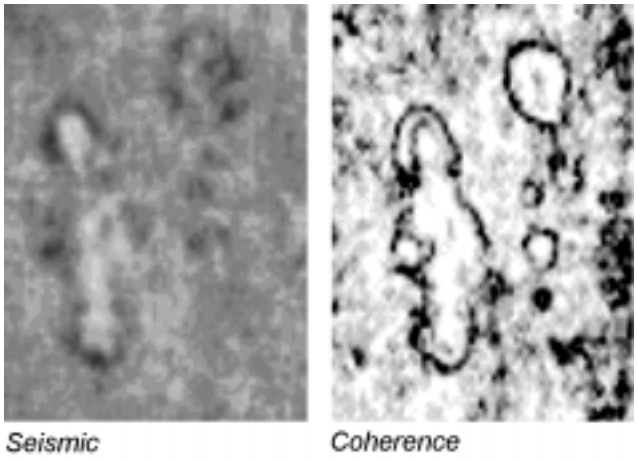

Figure 2 Boundaries of reefs seen distinctly on the coherence slice.

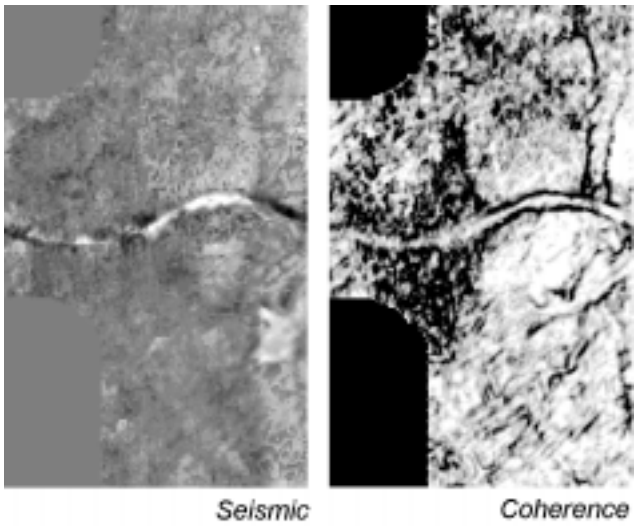

Figure 3 Channels seen clearly on the coherence slice.

reflector at each analysis point. The semblance can be interpreted as the ratio of the energy of the average trace within the analysis window to the average energy of the independent traces. Using this measure, if there is no spatial amplitude or waveform variation across the analysis window, the coherence will be equal to one. If the traces are random, or otherwise have polarity changes that give rise to a zero average trace, the coherence will be equal to zero. In general, a spatial analysis window of five traces provides maximum lateral resolution, but may be more susceptible to noise, such as acquisition footprint and migration artefacts. If these undesired features cannot be eliminated through reprocessing of the data, we can partially suppress them by using a larger spatial analysis window. Temporal analysis windows greater than 50 ms allow us to 'stack' the discontinuities associated with vertical faults, while temporal analysis windows of less than 20 ms avoid blending or mixing stratigraphic discontinuities from geological features above and below the horizon of interest. For this reason, it is valuable to have more than one coherence cube to consider.

The third-generation coherence algorithm is based on eigenstructure decomposition (Gersztenkorn & Marfurt 1999). In general, the reflector dip/azimuth are obtained from smoothed estimates obtained by the more computationally efficient semblance algorithm (Marfurt *et al.* 1999). We then 'flatten' the data in each analysis window, form a covariance matrix between the traces, and calculate the largest eigenvalue. The eigenvector corresponding to this largest eigenvalue defines a relative trace-to-trace amplitude variation along the reflector that best fits the data for all time samples within the analysis window. Physically, data represented by a single eigenvector will have arbitrary amplitude variation but identical waveform within the analysis window. Given this interpretation, we define the eigenstructure estimate of coherence as the ratio of the energy that can be represented by this eigenvector to the energy of the independent traces.

Given these definitions, we see that both the semblance and eigenstructure measures of coherence have their strengths and weaknesses. The eigenstructure algorithm is sensitive only to waveform, not amplitude variation, and will in general provide a sharper delineation of discontinuities. However, the eigenstructure algorithm degenerates as the temporal analysis window becomes smaller, when it becomes increasingly easy to fit 'all' the data in the window with a single spatial amplitude variation. As the temporal analysis window becomes one sample thick, the eigenstructure analysis of coherence always gives an estimate of one. In contrast, the semblance algorithm provides valuable images of stratigraphic discontinuities for an analysis window even when it is only one sample thick.

It must be emphasized that it is important to estimate coherence along some measure of reflector dip/azimuth. Figure 4 shows a time slice from a coherence volume where the analysis was performed with an implicit assumption of flat

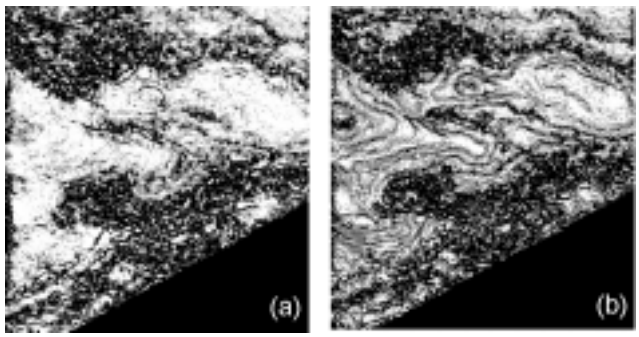

Figure 4 (a) Eigendecomposition algorithm. (b) Modified eigendecomposition algorithm.

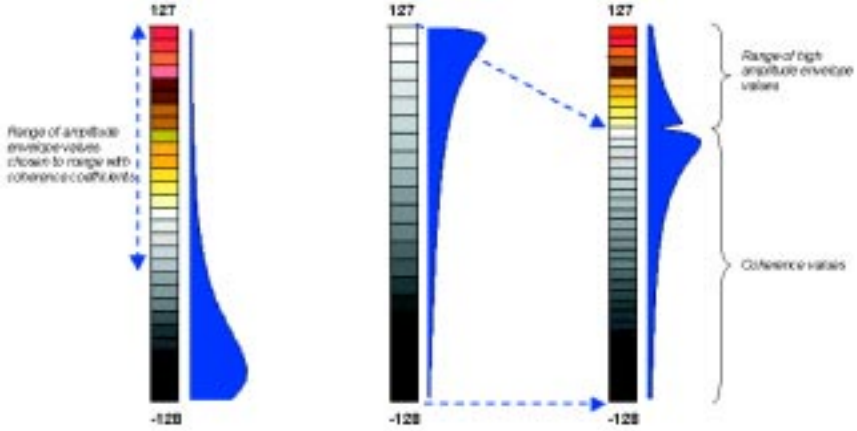

Figure 5 Mechanism of composite displays for amplitude envelope and coherence.

dip. On the left, we note artefacts (sometimes called structural leakage) following structural contours on our coherence image that complicate our interpretation. We show the same time slice on the right, where we have correctly calculated coherence along a non-zero estimate of dip/azimuth – we now see the faults clearly, uncontaminated by structural artefacts. It is of course possible, and for careful reservoir characterization studies perhaps desirable, to estimate our reflector dip/azimuth by manually picking (Marfurt *et al.* 1999) a real or phantom horizon of interest.

Attribute composite displays

Complex trace seismic attributes – including a measure of seismic amplitude, frequency and phase – have been successfully used in mapping lithology changes in the last two decades. During the computation of coherence using the semblance method, it is possible to obtain a smoother and more robust multitrace estimate of the complex trace attributes (Marfurt *et al.* 1998). Attributes are calculated during the coherence computation process within the predefined aperture using an ensemble of traces. For example, the amplitude envelope is calculated on the amplitudes with the highest coherence of the local waveform rather than a single trace response. While such attribute volumes can be used individually, it is possible to generate convenient composite displays. Occasionally on coherence slices, high coherence envelope amplitudes within channels, point bars or reefs are encountered. For ease of identification and corroboration, another coherence volume is created which has the coherence coefficients intact, but the high-end amplitudes from the coherence envelope volume are superimposed on it. Figure 5 illustrates how the high end of the amplitude envelope values is merged with coherence coefficients.

The high envelope amplitudes corresponding to the events of interest stand out as 'bright spots' on coherence slices. Figure 6 shows the composite displays for the reef and channel features shown in Figs 2 and 3. Such displays help not only in identification of the nature and extent of depositional features but also in gaining an understanding of the depositional environment.

The coherence cube offers a high-resolution unbiased image of the variations within the volume, wherein geological features and faults are enhanced. The inverted seismic volume, e.g. the acoustic impedance volume, exhibits an improved image of the impedance variations which can be used for lithological and stratigraphic interpretation. By integrating the coherence and impedance volumes, acoustic impedance changes can be readily identified within sedimentary systems, resulting in unparalleled detail of subtle sedimentary depositional features (Chopra 2001). Acoustic impedance results may be combined numerically with the coherence results, producing a volume that allows the interpreter to display the stratigraphic images from the 3D seismic data and examine the acoustic impedance contrast across them. For example, sand deposition within a channel that is gas-charged would

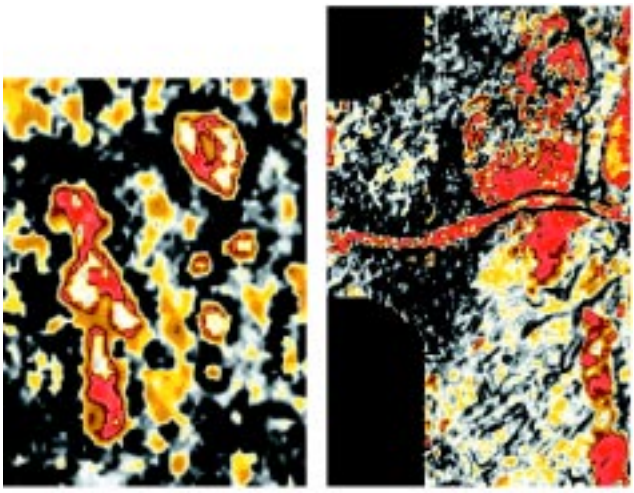

Figure 6 Composite displays depicting the high end of envelope amplitudes superimposed on coherence (see Figs 2 and 3).

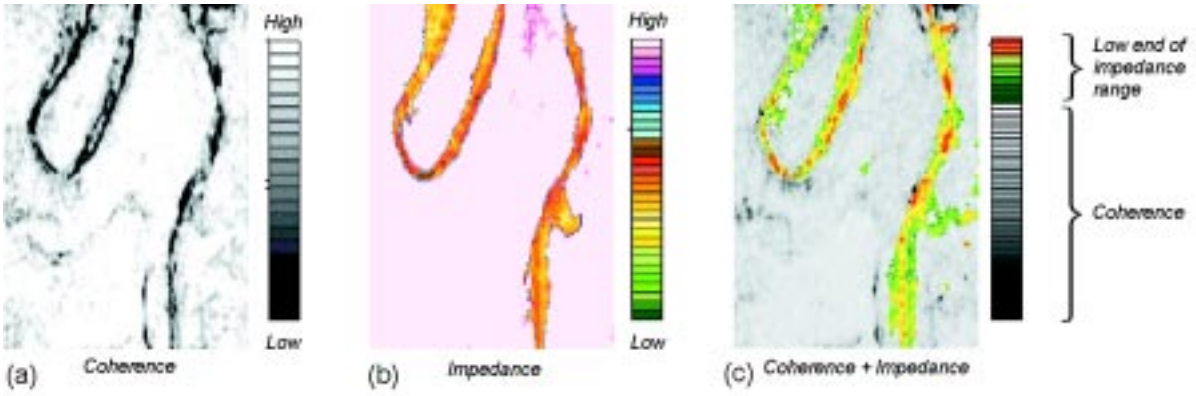

Figure 7 Time slices from different volumes.

exhibit a low impedance, so a range of low impedance representing the gas sands may be selected and merged with the coherence cube. The composite merged volume thus generated may again be sliced through to see low impedance (in colour) displayed within the boundaries of the channel.

Channel sand reservoirs are difficult to develop efficiently, but they often have excellent production characteristics. The depositional mechanisms involved in channels can create sandbodies whose thickness and quality can vary rapidly over short distances. Such rapid variations make it difficult to use conventional seismic data successfully for mapping. Impedance inversion helps in such cases.

Figure 7a shows a coherence slice depicting two channels that stand out clearly in a high-coherence background. The impedance slice (Fig. 7b) indicates low impedance within the channels, implying the presence of hydrocarbon-bearing sands. A composite volume may be generated, wherein the low end of the impedance amplitudes is merged with the coherence coefficients (Chopra 2001). When stretched over a suitable colour scale (Fig. 7c), the variation within the low end of the range of the impedance values chosen is clearly seen within the boundaries of the channel.

Such composite plots can be used for a convincing definition of precise reservoir and non-reservoir facies boundaries and reservoir compartments.

Acquisition footprint detection and removal

Acquisition footprint is a term used to define grid patterns of different shapes seen on 3D seismic time slices that tend to 'mirror' parts of the acquisition geometry used for shooting the seismic survey. They are usually seen on shallow time slices or horizon amplitude maps as striations masking the actual amplitude anomalies under consideration or stratigraphic interpretation. Apart from the acquisition footprints, processing artefacts can also result in prominent lineations on the seismic slices that prevent the accurate mapping of amplitudes. Such patterns have an adverse effect on any subsequent special processing that may be undertaken. For example, the inverted impedance volumes would carry undesirable striping on the slices.

Although acquisition footprints need to be considered at the time of survey planning, their removal can be effected at the time of processing. Coherence affords an elegant tool for detecting the footprints during the processing flow and for then deciding on the most accurate way they can be attenuated (Chopra & Larsen 2000). As seen in Fig. 8, acquisition footprints show up clearly on the coherence slice but are not so obvious on the seismic time slice. Thus it can be checked that they have been removed effectively.

Fault/fracture detection

The interpretation of faults can be carried out on 3D seismic data volumes if their location and throws are discernible. Small faults have a minute reflector offset that in most cases appears as an inconsequential disruption. Minor faults are usually not detected directly on the seismic volumes, although indirect evidence (from well data or the geological setting of the subsurface) does suggest the existence of faults and fractures in the area. A plausible reason for this is that, although the seismic data acquisition is designed to record a wide range of azimuths, the stacking process obliterates this information. A new method has been devised (Chopra *et al*. 2000) for detecting such faults and fractures in 3D seismic data by taking advantage of the azimuthal variation of seismic signatures and coherence. It consists of trapping off a restricted azimuth range from the full 3D seismic wavefield so that azimuthal variation of moveout and amplitude is not obliterated. Appropriate steps are taken to ensure an adequate offset and azimuth distribution within the individual subvolumes, which are then examined using coherence.

After the application of surface-consistent statics and zero-phase deconvolution to the CDP gathers, they are binned into four different azimuth volumes according to the direction be-

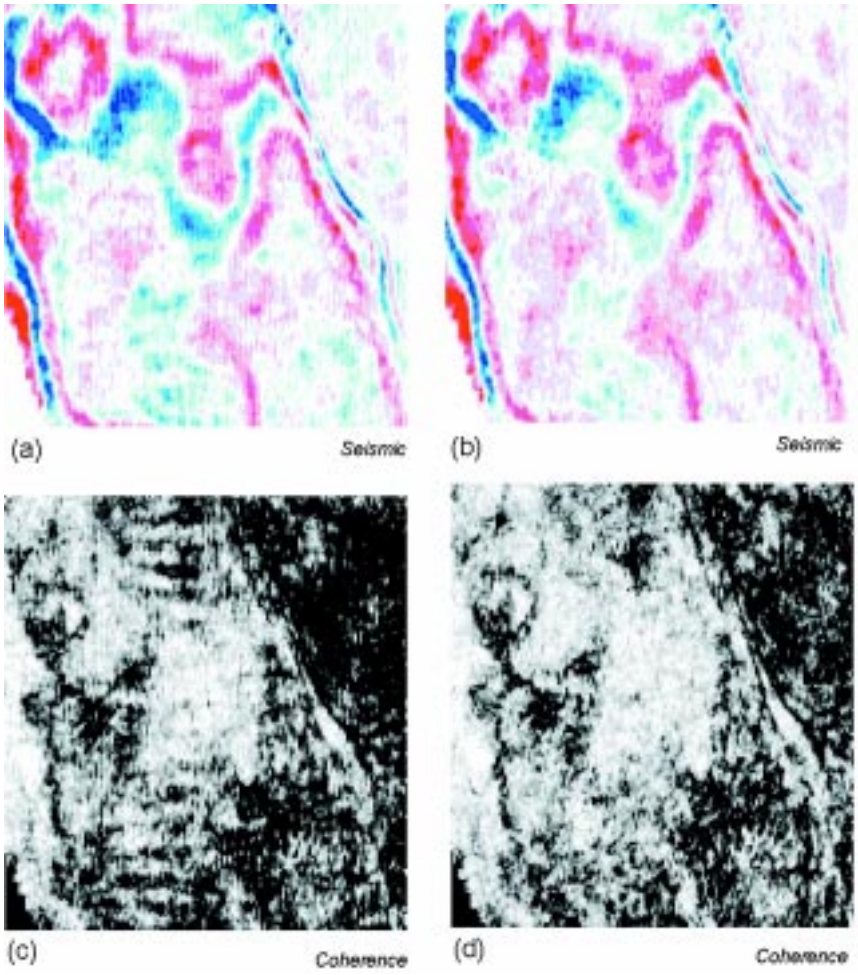

Figure 8 Time slices from seismic and coherence volumes (left) before and (right) after acquisition footprint removal.

tween source and receiver, but within 45° of the dominant fault strike. The data set chosen for the example analysis is an OBC volume with an offset multiplicity of about 60. The ranges of azimuths fixed for the four volumes are 45–90°, 90–135°, 135–180° and 180–225°. Thereafter, processing was carried out independently for each of the four volumes. This included the following steps: spatially de-aliasing dip moveout (DMO) (Beasely & Mobley 1997), velocity analysis, stacking and migration.

To ensure that DMO preserved the seismic amplitudes, a number of issues had to be addressed: the binning of the input data to ensure that the offset classes were balanced, the spatial sampling of the DMO operator, and the DMO-orientated weighting of the DMO stack to compensate for the effects of the acquisition geometry on the stack amplitudes. A comparison of individual velocity analyses indicated changes related to azimuthal anisotropy.

The different azimuth subvolumes were analysed using coherence. Coherence cubes were run on them using the modified eigendecomposition algorithm, a five-sample eigenoperator and a spatial radius equal to a bin length.

As expected, there was variation in the reflection event distribution and more detail in the restricted azimuth sections, compared with the conventional sections. Figure 9 shows the time slices at 1312 ms from the coherence volumes. Some NE–SW faults are seen on the conventional time slice but are not very distinct. Different azimuth coherence slices exhibit better alignment not only in the NE–SW direction but also in the orthogonal direction. A distinct cross fault is seen on the 157.5–202.5° azimuth volume.

An important observation is that despite significantly lower fold of the restricted azimuth volumes, superior imaging is seen in the fracture-perpendicular direction. This result is intuitive to standard practices and suggests that both the fault-parallel and fault-perpendicular volumes need to be analysed for accurate fault interpretation.

This methodology could be very significant in the identification of zones where productivity is influenced by fractures and faults.

Sharpened coherence cubes

It is possible to extract more detail out of the coherence cube

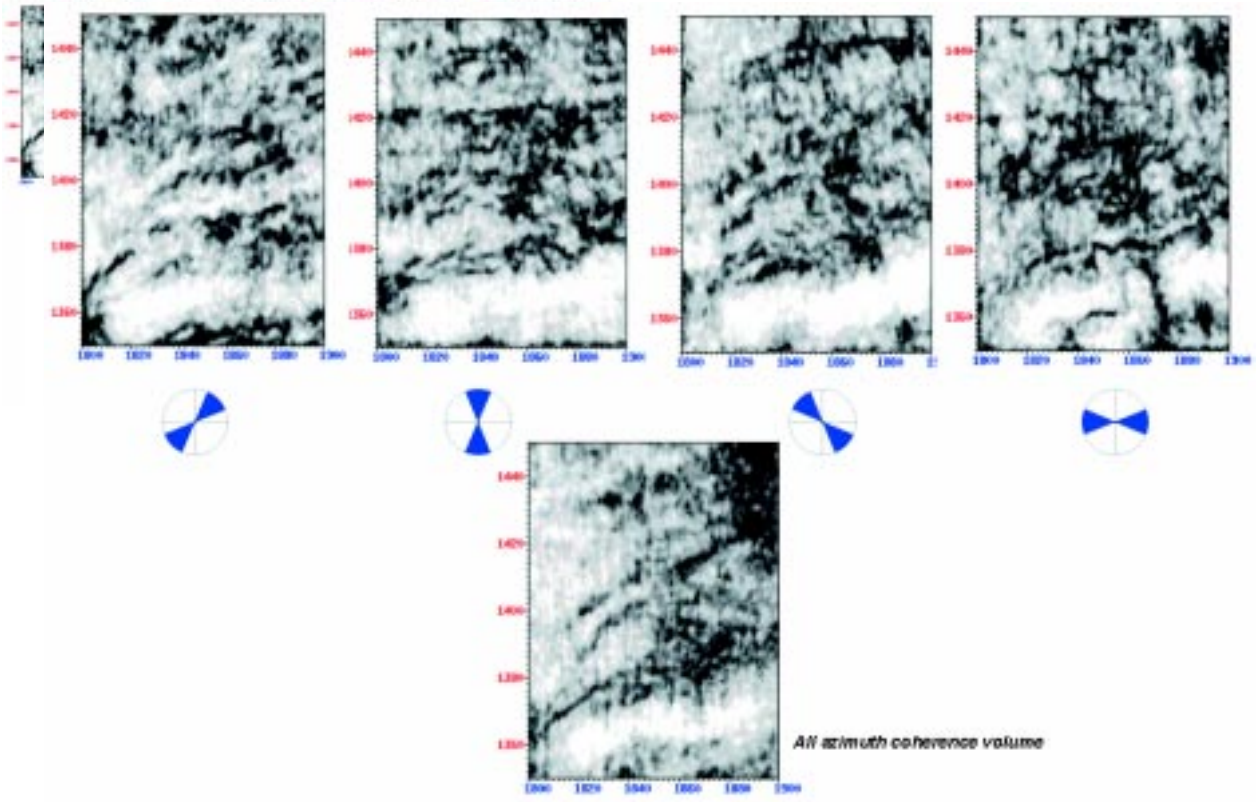

Figure 9 Time slices from different azimuth-restricted coherence volumes and the all azimuth coherence volume.

slices. A new algorithm (proprietary to Scott Pickford) that combines the eigendecomposition of covariant matrices and edge enhancement operators can be applied to the 3D seismic data. The action of this algorithm can be appreciated better by drawing an analogy with the FX DECON process run on post-stack data. Usually, a certain percentage of noise level is added to the data to prevent the seismic section from appearing artificial. In the same way, the effect of the algorithm is similar to taking a certain percentage of the low coherence values and adding them to the range of coherence values. This

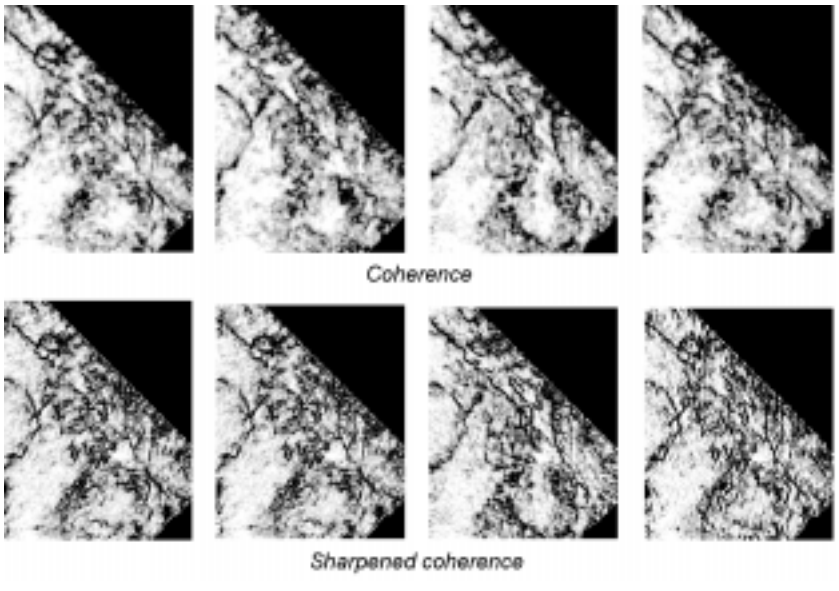

Figure 10 Comparison of coherence and sharpened coherence slices.

accentuates the discontinuities and gives them a sharpened appearance. The output is a 3D cube of sharpened coherence coefficients (Chopra & Sudhakar 2000). Apart from a straightforward computation of the sharpened coherence cube, it is possible to impart a weak directional bias during the sharpening process, which tends to accentuate the fault or fracture lineations. Figure 10 depicts a set of coherence slices and a corresponding set of slices from the sharpened coherence volumes with directional bias. It is evident that faults can be tracked easily on such displays and their mapping could be performed conveniently and accurately.

Complimentary processing tool

Integration of coherence cube imaging into the seismic processing flow produces optimal images of the subsurface. Coherence cube processing is used at different steps to effect the optimum choice of processing parameters, noise reduction methods or migration velocities. For example, coherence cubes are generated for a range of migration velocities and those velocities chosen that best image the data.

Coherence – a promising tool

Following extensive and successful testing in different basins around the world, coherence processing has evolved and developed into an indispensable tool, which effectively extracts a vast amount of information from 3D seismic data volumes that would otherwise be overlooked. Not only does it provide the interpreter, the geologist and the reservoir engineer with a valuable tool that significantly increases productivity and accuracy, but it also yields a better input for reservoir models and reduces the risks associated with drilling locations.

Acknowledgements

I am indebted to Kurt Marfurt for rewriting the section on algorithms and for other discussions that have benefited this paper. I also thank Scott Pickford for permission to publish this paper. Coherence Cube is a trademark of Core Laboratories.

References

Bahorich, M. and Farmer, S. [1995] The coherence cube. *The Leading Edge* **14**, 1053–1058.

Beasely, C.J. and Mobley, E. [1997] Spatial dealiasing of 3D DMO. *67th Meeting, Society of Exploration Geophysicists*, Expanded Abstracts.

Chopra, S. [2001] Integrating coherence cube imaging and seismic inversion. *The Leading Edge* **20**, 354–362.

Chopra, S. and Larsen, G. [2000] Acquisition footprint – its detection and removal. *CSEG Recorder* **25**(8), 16–20.

Chopra, S. and Sudhakar, V. [2000] Fault interpretation – the coherence cube and beyond. *Oil and Gas Journal* **31 July**, 71–74.

Chopra, S., Sudhakar, V., Larsen, G. and Leong, H. [2000] Azimuth based coherence for detecting faults and fractures. *World Oil* **September**, 57–62.

Gersztenkorn, A. and Marfurt, K.J. [1999] Eigenstructure based coherence computations as an aid to 3-D structural and stratigraphic mapping. *Geophysics* **64**, 1468–1479.

Marfurt, K.J., Kirlin, R.J., Farmer, S.L. and Bahorich, M.S. [1998] 3-D seismic attributes using a semblance-based coherency algorithm. *Geophysics* **63**, 1150–1165.

Marfurt, K.J., Sudhakar, V., Gersztenkorn, N.A., Crawford, K.D. and Nissen, S.E. [1999] Coherency calculations in the presence of structural dip. *Geophysics* **64**, 104–111.